

Vibrational assignment, structure and intramolecular hydrogen bond of 4-methylamino-3-penten-2-one

Heidar Raissi*, Effat Moshfeghi, Farzaneh Farzad

Chemistry Department, Birjand University, Birjand, Iran

Received 9 February 2005; received in revised form 4 April 2005; accepted 6 April 2005

Abstract

The molecular structure, intramolecular hydrogen and vibrational frequencies of 4-methylamino-3-penten-2-one were investigated by a series of density functional theoretical (DFT) calculations and ab initio calculation at the post-Hartree–Fock (MP2) level. Fourier transform infrared and Fourier transform Raman spectra of this compound and its deuterated analogue were clearly assigned. The calculated geometrical parameters show a strong intramolecular hydrogen bond with a N···O distance of 2.622–2.670 Å. This bond length is about 0.02 Å shorter than that in its parent, 4-amino-3-penten-2-one which is in agreement with spectroscopic results. Furthermore, the conformations of methyl groups with respect to the plane of the molecule and with respect to each other were investigated.

© 2005 Elsevier B.V. All rights reserved.

Keywords: Intramolecular hydrogen bond; Aminoketone; 4-methylamino-3-penten-2-one; Vibrational spectra; α,β -Unsaturated- β -ketoenamine

1. Introduction

Hydrogen bonding is an important phenomenon in many chemical and biological systems, and hydrogen bonding complexes have been extensively studied by a wide range of experimental techniques and calculations [1–10]. Studies on intramolecular hydrogen bonding have become increasingly popular in the past [10–20]. These systems are attractive because they have a quite high thermodynamic stability and a uniform structure [20–23]. The stability of intramolecularly hydrogen-bonded complexes allows performing experimental studies in a wide range of temperatures and solvents. The keto-amine form of α,β -unsaturated- β -ketoenamines are stabilized by a strong intramolecular hydrogen bond (N–H···O) [1,2,24,25]. The heteronuclear N–H···O is even more important than the homonuclear O–H···O bond because of its outstanding importance in protein folding and DNA pairing and its even-growing application in molecular recognition and crystal engineering problems [26–28]. The vibrational spectra of α,β -unsaturated- β -ketoenamines have been the subject of few investigations [1,2,25], which support the existence of

a strong intramolecular hydrogen bond of chelating nature of keto-amine form of these compounds. This hydrogen bond formation leads to an enhancement of the resonance conjugation of the π -electrons, which causes a marked tendency for equalization of the bond orders of the valence bonds in the resulting six-member chelated ring. Therefore, it seems that any parameter that affects the electron density of the chelated ring will change the hydrogen bond strength.

In the previous work [1], we showed that the strength of such a bridge enhances when an electron-withdrawing group replaces the H atom in α position (position 3 in Fig. 1), the same as β -diketones [29]. In the case of β -diketones, several experimental data suggests that the hydrogen bond becomes stronger when bulky or electron-releasing groups are involved in β -position [30,31]. By analyzing the substitution effect of simple substitutes such as methyl group, an electron-releasing group with the steric effect on the structure, it is possible to study the inductive and steric effects for this kind of substitution. Yet, the effect of substitution on the nitrogen atom (see Fig. 1) of ketoenamines has been investigated neither experimentally nor theoretically.

A crystalline derivative of 4-amino-3-penten-2-one (hereafter APO) is 4-methylamino-3-penten-2-one (hereafter MeAPO). The solubility of this compound is low and crystal-

* Corresponding author. Tel.: +98 561 2224803; fax: +98 561 8438032.
E-mail address: hraeisi@birjand.ac.ir (H. Raissi).

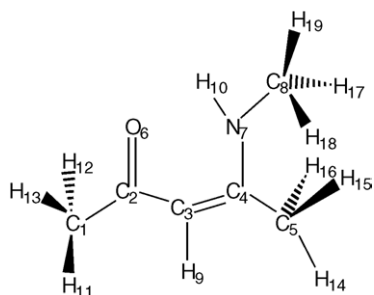


Fig. 1. View of MeAPO showing the atomic numbering scheme used in the text.

lized spontaneously during preparation. MeAPO is an interesting compound among the substituted APO derivatives so far investigated. It has a relatively simple structure, at ambient temperature it is solid and this compound is only involved in intramolecular hydrogen bond. Whereas, in the case of APO, experimental evidences indicate presence of an intermolecular hydrogen bond in the solid state, completely, and in solution partially [2].

The aim of the present paper is to predict the structure and vibrational spectra (harmonic wavenumbers, and relative intensities for Raman and IR spectra) of MeAPO by means of density functional theory (DFT) levels. Comparing of MeAPO and APO geometrical parameters gives a clear understanding of substitution effects of hydrogen atom with methyl group (on N atom) on structure and hydrogen bond strength of the system. The calculated harmonic force constants of MeAPO were used for predicting the Raman and IR spectra of deuterated species. The calculated vibrational frequencies are compared with the obtained experimental results.

2. Experimental

Acetylacetone and all solvents were purchased from Fluka. Chloroform and deuterated chloroform were stored over 3 Å molecular sieves.

The concentration of the samples for ^1H NMR and FTIR measurements was 0.1 mol dm^{-3} .

MeAPO was synthesized by the modification of the method given for APO in Ref. [32].

The amount of 10 g (0.1 mol) acetylacetone was dissolved in 60 cm^3 methylamine solution 40%, refluxed for 4 h and then stirred continuously for 24 h at room temperature. Mixture was extracted ($3 \times 100 \text{ ml}$) with chloroform. Organic layer was dried using anhydrous Na_2SO_4 , filtered and evaporated under reduced pressure. The crude product was crystallized from CHCl_3 . Yield 6.1 g (61%) of colorless crystals; m.p. 39.9°C , literature $39\text{--}40^\circ\text{C}$, ^1H NMR (CDCl_3): δ 1.91 (s, 3H, CH_3), δ 1.99 (s, 3H, CH_3), δ 2.94 (s, 3H, CH_3), δ 4.98 (s, 1H, CH_α) and δ 10.7 (s, 1H, NH bonded). The elemental analysis was correct.

Solution of DMeAPO (deuteration done on amine proton) was prepared by shaking solution of MeAPO in CCl_4 with D_2O for period of up to 24 h. However, the crystalline DMeAPO was prepared from CCl_4 solution of DMeAPO which was dried over anhydrous Na_2SO_4 followed by removing the organic layer under reduce pressure.

The infrared spectra were taken on a Nicolet 800 spectrometer. The Raman spectra were collected employing a 180° back scattering geometry and a Nicolet 910 Fourier Transform Raman spectrometer.

The Raman spectrometer was equipped with a ZnSe beam splitter and a liquid N_2 cooled germanium detector. Rayleigh filtering was afforded by a set of two holographic technology filters. Laser power at the sample was 40 mW. The NMR spectra were obtained on a FT-NMR, Bruker Aspect 3000 spectrometer at 100 MHz frequency in CDCl_3 at 22°C and TMS as internal standard.

3. Method of analysis

It is well known that an adequate treatment of electronic correlation effects is important in calculations on H-bonded species [33]. In the present study, the molecular equilibrium geometry, vibrational frequencies and infrared and Raman intensities were computed with the GAUSSIAN98W software system [34] by using a selection of modern density functional and ab initio MP2 level. The B [35] or B3 [36] or G96 [37] exchange functional were combined with the PW91 [38] or LYP [39] correlation functionals, resulting in the four different functionals BLYP, G96LYP, B3PW91 and B3LYP. A series of calculation on MeAPO were performed with medium size 6-31G* (142 basis functions, 268 primitive Gaussians) and 6-31G** (175 basis functions, 301 primitive Gaussians) basis sets. Application of the B3LYP, BLYP and G96LYP density functional was repeated with the larger basis set, 6-311++G** (253 basis functions, 387 primitive Gaussians).

4. Results and discussions

4.1. Molecular geometry

The molecular equilibrium geometry predicted with the B3LYP, B3PW91, BLYP, G96LYP density functionals and ab initio MP2 level are given in Table 1. The geometry of MeAPO and the numbering of the atoms is given in Fig. 1. It is apparent that replacement of the PW91 correlation functional with the LYP functional leads to the prediction of a shorter $\text{O} \cdots \text{H}$ distance, corresponding to a more symmetrical H-bond. A somewhat similar tendency is observed when G96 functional is replaced by the B3 and B hybrid exchange functionals. On the other hand, the main effect of methyl substitution on the nitrogen atom is shortening of the $\text{N} \cdots \text{O}$ distance and lengthening of the N–H bond length, compared with the corresponding value for APO [1,2]. Calculations

Table 1
Comparison of theoretical geometric parameters of MeAPO at different levels of theory

	B3LYP ^a	G96LYP ^a	B1LYP ^a	B3LYP ^b	B1LYP ^b	G96LYP ^b	B3PWP91 ^b	B3LYP ^c	B1LYP ^c	G96LYP ^d	MP2 ^a
Bond lengths											
C ₃ –C ₄	1.386	1.398	1.382	1.387	1.385	1.399	1.385	1.386	1.385	1.397	1.380
C ₂ –C ₃	1.437	1.442	1.441	1.436	1.436	1.441	1.434	1.436	1.436	1.439	1.439
C ₂ –O ₆	1.250	1.266	1.246	1.251	1.248	1.267	1.249	1.247	1.244	1.262	1.255
C ₄ –N ₇	1.348	1.358	1.350	1.347	1.347	1.357	1.343	1.346	1.345	1.355	1.350
C ₁ –C ₂	1.523	1.534	1.523	1.522	1.522	1.533	1.516	1.519	1.519	1.539	1.516
C ₄ –C ₅	1.506	1.515	1.507	1.506	1.506	1.514	1.501	1.504	1.505	1.513	1.503
C ₃ –H ₉	1.084	1.090	1.083	1.083	1.082	1.089	1.084	1.081	1.080	1.087	1.085
N ₇ –H ₁₀	1.026	1.039	1.021	1.027	1.024	1.042	1.029	1.024	1.021	1.036	1.023
N ₇ –C ₈	1.448	1.457	1.448	1.448	1.448	1.457	1.442	1.451	1.451	1.460	1.448
O ₆ ···H ₁₀	1.806	1.778	1.839	1.783	1.799	1.748	1.756	1.815	1.828	1.793	1.837
O ₆ ···N ₇	2.655	2.656	2.675	2.640	2.648	2.637	2.622	2.655	2.660	2.660	2.670
dc–c–dc=c	0.0509	0.0438	0.0587	0.0495	0.0516	0.042	0.0482	0.0496	0.0518	0.0425	0.0585
Bond angles											
C ₄ –C ₃ –C ₂	123.0	123.1	123.3	122.8	122.8	122.8	122.5	123.2	123.2	123.3	123.1
C ₃ –C ₂ –C ₁	118.3	118.5	117.23	118.4	118.3	118.7	118.2	118.4	118.4	118.5	117.2
C ₃ –C ₄ –C ₅	120.9	121.2	120.83	120.1	120.9	121.2	121.1	120.8	120.7	121.0	121.0
N ₇ –C ₄ –C ₃	121.2	120.4	121.5	121.0	121.2	120.2	120.8	121.3	121.5	120.6	121.8
C ₃ –C ₂ –O ₆	123.5	123.4	123.6	123.4	123.4	123.3	123.4	123.2	123.2	123.2	123.6
C ₄ –N ₇ –H ₁₀	112.9	112.1	113.3	112.7	112.9	111.7	112.3	113.4	113.6	112.5	113.6
C ₄ –N ₇ –C ₈	126.1	126.6	126.1	126.0	126.0	126.5	126.0	126.0	126.0	126.5	125.5
N ₇ –C ₄ –C ₅	117.8	118.3	117.6	118.0	117.9	118.5	118.1	117.9	117.8	118.3	117.2
C ₈ –N ₇ –H ₁₀	120.9	121.2	120.5	121.3	121.0	121.8	121.7	120.6	120.3	121.0	120.8
C ₂ –C ₃ –H ₉	119.0	119.0	118.6	119.1	119.0	119.2	119.2	118.9	118.9	118.9	118.7
O ₆ –C ₂ –C ₁	118.1	118.0	119.1	118.1	118.2	118.0	118.4	118.4	118.4	118.3	119.2
N ₇ –H ₁₀ –O ₆	137.6	139.5	136.6	138.3	137.7	140.5	139.1	136.7	136.2	138.5	136.1

^a Calculated with 6-31G* basis set.

^b Calculated with 6-31G** basis set.

^c Calculated with 6-311++G** basis set.

at all computational levels predict that the N···O distance in MeAPO is about 0.02 Å shorter than that in APO. These structural changes in MeAPO suggest a stronger hydrogen bond in MeAPO than that in APO [1,2]. This conclusion is consistent with the NMR proton chemical shift of 9.7 and 10.7 ppm for the hydrogen-bonded proton in APO and MeAPO, respectively. On the other hand, upon methyl substitution on the nitrogen atom both C=C and C=O bond lengths are increased whereas C–C and C–N bond lengths are decreased (in comparison to APO). Lengthening of double bonds and shortening of single bonds could be attributed to increasing of α -electrons delocalization in the chelate ring of MeAPO, which in turn causes the hydrogen bond become stronger than APO.

An interesting point, which is noteworthy, is the planarity of the chelated ring in MeAPO (the same as APO), which is caused by the formation of a strong intramolecular hydrogen bond and π -electron conjugation in the chelated ring. According to all calculations, the hydrogen of NHCH₃ group is completely in the plane of the chelated ring. This implies that the electron lone pair of the nitrogen atom is almost completely takes part in the π -electron delocalization of the chelated ring.

The conformations of methyl groups with respect to the plane of the molecule and with respect to each other are shown in Fig. 2. The energy values and dihedral angles of these conformers are listed in Table 2. For each of the nine

geometries, the dihedral angles listed in Table 2 were held constant and all the remaining parameters were varied until the minimum energy was achieved. The dihedral angle ϕ_1 (H₁₄C₅C₄N₇) at the most stable conformation (1) is 180°, which is about 70 and 1700 cal/mol (calculated at B3LYP/6-31G** level) more stable than the eclipsed (5) and staggered (4) conformers, respectively. However, the dihedral angle ϕ_2 (H₁₉C₈N₇C₄) at the most stable conformation (1) is 179.7°, which is only 0.37 cal/mol (calculated at B3LYP/6-31G** level) more stable than the eclipsed conformer (6). The calculated barrier to rotation for the CH₃ attached to the carbonyl group and the CH₃ attached to the nitrogen atom are about 53 and 592 cal/mol (calculated at B3LYP/6-31G** level), respectively.

4.2. Vibrational analysis

The fundamental vibrational frequencies for MeAPO obtained at MP2 level and different DFT levels were compared with the experimental values by means of regression analysis. The superior quality results are produced from the B3LYP level. In the regression analysis a set of 48 vibrational bands was selected, corresponding to fundamentals numbers: ν_1 – ν_{48} . The regression parameters, linear correlation coefficient, *R*-square and standard deviation (S.D.), are listed in Table 3. As it is obvious in this table, the best results are obtained with B3LYP, resulting in S.D. = 13.49

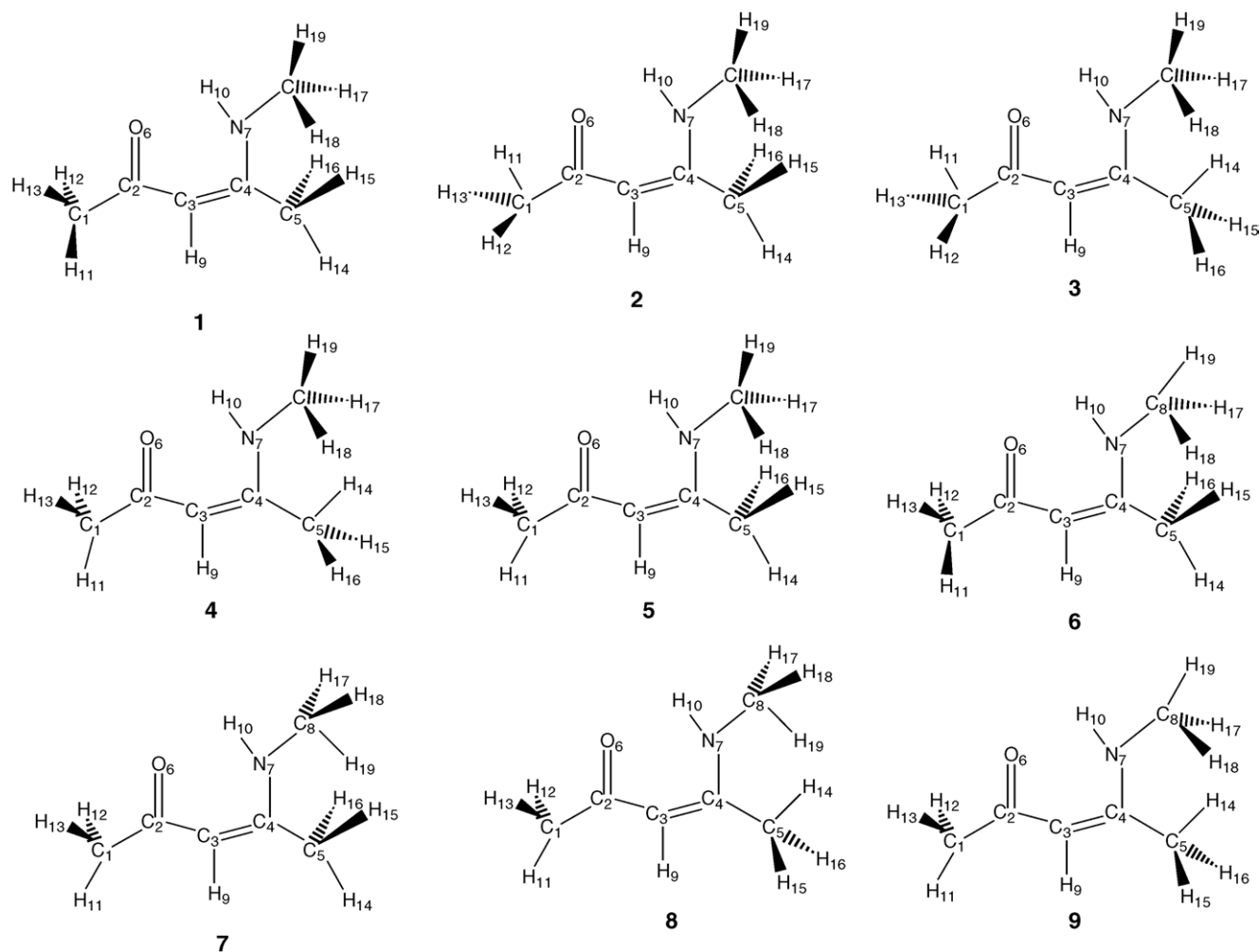


Fig. 2. Conformations of MeAPO optimized at B3LYP/6-31G** level.

and 15.81 cm^{-1} for B3LYP/6-31G** and B3LYP/6-31G*, respectively. It is noteworthy that any of the present DFT calculations leads to better correlation with experimental wavenumbers than the more time-consuming MP2 procedure (Table 3).

The Raman spectra of MeAPO and DMeAPO in the solid phase are shown in Fig. 3. Lorentzian function has been utilized for deconvolution [2,3,40,41] of the IR spectra of MeAPO in the solution phase in $3200\text{--}2800\text{ cm}^{-1}$ region and deconvoluted spectrum is shown in Fig. 4. The deconvoluted IR spectra of MeAPO and DMeAPO in the CCl_4 solution in $1800\text{--}800\text{ cm}^{-1}$ region are shown in Figs. 5 and 6, respectively. The infrared and Raman band frequencies for MeAPO and DMeAPO in the solid phase and in CCl_4 solution along with the calculated frequencies and their assignments are given in Tables 4 and 5, respectively. All calculated frequencies at different levels and basis sets are compared in Table 6.

The calculated frequencies are slightly higher than the observed values for the majority of the normal modes. Two factors may be responsible for the discrepancies between

the experimental and computed spectra of MeAPO and DMeAPO. The first is caused by the environment. The second reason for these discrepancies is the fact that the experimental value is an anharmonic frequency while the calculated value is a harmonic frequency.

4.3. Band assignment

The band assignment presented here obey the following criteria: (a) the observed band frequencies and intensity changes in the infrared and Raman spectrum of the deuteration analogue confirmed by establishing one to one correlation between observed and theoretically calculated frequencies. (b) Comparison in some cases with reported vibrational assignment of characteristic molecular groups and bond found in different molecules. (c) The visual 3D computerized representation of the normal modes.

4.3.1. $3600\text{--}1700\text{ cm}^{-1}$ region

In this region, CH stretching of the CH_3 groups, olefinic CH stretching and the NH/ND stretching are expected to be observed.

Table 2
The energies and dihedral angles (°) of MeAPO conformers given in Fig. 3

	1	2	3	4	5	6	7	8	9
H ₁₁ C ₁ C ₂ O ₆	174.3	0.0	0.0	180.0	180.0	174.3	180.0	180	180
H ₁₃ C ₁ C ₂ O ₆	52.3	-120.7	-120.7	59.7	59.7	52.3	59.7	59.7	59.7
H ₁₂ C ₁ C ₂ O ₆	-64.4	120.8	120.8	-59.5	-59.5	-64.4	-59.7	-59.5	-59.5
H ₁₄ C ₅ C ₄ N ₇	180.0	180.0	0.0	180.0	180.0	180.0	180	0	0
H ₁₅ C ₅ C ₄ N ₇	59.7	59.7	-120.7	-120.7	59.7	59.7	59.7	120.8	120.8
H ₁₆ C ₅ C ₄ N ₇	-59.5	-59.5	120.8	120.8	-59.5	-59.5	-59.8	-120.7	-120.7
H ₁₇ C ₈ N ₇ C ₄	-61.1	-61.1	-61.1	-61.1	-61.1	-61.1	-120.8	-120.8	-61.1
H ₁₈ C ₈ N ₇ C ₄	60.0	60.0	60.0	60.0	60.0	61.1	120.7	120.7	61.1
H ₁₉ C ₈ N ₇ C ₄	179.7	179.7	179.7	179.7	179.7	180.0	0.0	0.0	180.0
Energy (a.u.) ^a	-365.256655	-365.25657	-365.255712	-365.25394	-365.25654	-365.2566546	-365.2557116	-365.2524412	-365.2539357
Relative to I (kcal/mol) ^a	0.0	0.053981	0.592620	1.70751	0.070309	0.00037	0.59262	2.645402	1.707194
Energy (a.u.) ^b	-364.1180049	-364.1177652	-364.1148738	-364.1146761	-364.1176732	-364.1177864	-364.116645	-364.1125589	-364.1147194
Relative to I (kcal/mol) ^b	0.0	0.150096	1.960647	2.084444	0.207705	0.136821	0.851549	3.410202	2.057330

^a Calculated at B3LYP/6-31G**.

^b Calculated at MP2/6-31G**.

Table 3
Regression analysis of fundamental wavenumbers with theoretical corresponds

Levels	Linear correlation coefficient	R-square	Standard deviation
B3LYP/6-31G**	0.999899	0.999798	13.4952
B3LYP/6-31G*	0.999876	0.999753	15.81139
B1LYP/6-31G**	0.999856	0.999711	16.14094
B3PW91/6-31G**	0.999836	0.999672	17.20268
G96LYP/6-31G*	0.999816	0.999632	18.2163
B3LYP/6-311++G**	0.999792	0.999584	19.3781
G96LYP/6-311++G**	0.999781	0.999563	19.85902
G96LYP/6-31G**	0.999777	0.999554	20.06008
B1LYP/6-31G*	0.999774	0.999548	20.18144
B1LYP/6-311++G**	0.999755	0.999510	21.03194
MP2/6-31G*	0.999706	0.999411	23.04563

In the infrared and Raman spectra of MeAPO in the solid phase a medium band was observed at about 3165 cm⁻¹. In solution, this band slightly shifts to upper frequencies and appears at 3171 cm⁻¹. This band shows no intensity change on dilution. Upon deuteration, this band disappears and a new band appears at about 2275 cm⁻¹. According to the theoretical calculations, we assign this band to N–H (involved in an intramolecular hydrogen bond) stretching. The corresponding band for APO [2] is observed at about 3180 cm⁻¹. Lower band frequency shift of NH stretching mode in MeAPO in comparison with that for APO suggests stronger intramolecular hydrogen bond in MeAPO in comparison with that APO. The Raman spectrum of MeAPO shows a medium band at 3079 cm⁻¹. According to the calculation and in comparison with APO [2], this band is attributed to ν CH_α. The Raman spectrum of MeAPO and its deuterated analogue clearly shows seven bands at 3013, 2999, 2987, 2965, 2937, 2915 and

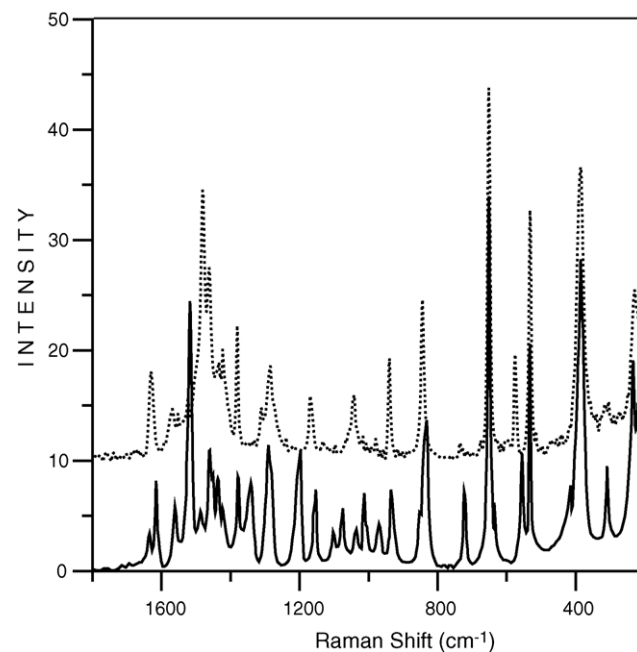


Fig. 3. Raman spectra of MeAPO (—) bottom) and DMeAPO (···) top).

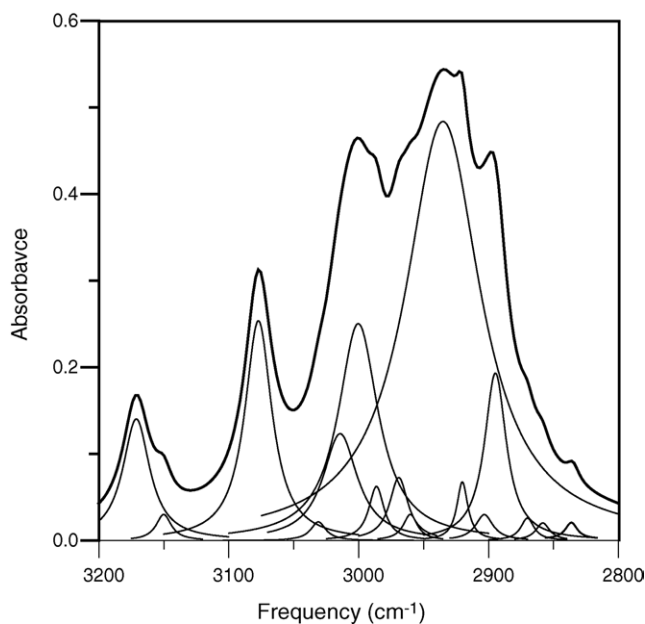


Fig. 4. Deconvoluted infrared spectrum of MeAPO in solid phase in 3200–2800 cm^{-1} region, the experimental spectra (top) and the results of fitting (bottom).

2885 cm^{-1} , which are very close to the corresponding bands observed in the Raman spectrum of APO [2] and therefore assigned to the CH_3 stretching modes. Furthermore, deconvolution of infrared spectrum of MeAPO shows another weak bands in this region (see Fig. 4). It seems that these bands are overtones of strong bands at 1700–1400 cm^{-1} region.

4.3.2. 1700–1000 cm^{-1} region

Beside the CH_3 deformation and rocking, N-CH_3 stretching and in plane CH_α bending modes, five bands are expected to be observed in this region in relation to the chelated ring modes which are attributed to C=O , C=C , C-C , C-N stretching and the N-H in-plane bending modes.

The infrared spectrum of MeAPO apparently shows only one band in the 1650–1600 cm^{-1} region. This band in the solid phase and in the CCl_4 solution appears at about 1615 cm^{-1} . However, by deconvolution of the infrared spectrum of MeAPO in this region a medium band appears at about 1640 cm^{-1} (see Fig. 5). The corresponding band in the Raman spectrum occurs at 1633 cm^{-1} , but its relative intensity is more than its corresponding band in APO [2], which occurs at 1623 cm^{-1} . Our normal mode analysis shows that this band is due to the asymmetric C=C-C=O stretching which is slightly coupled to δNH . Upon deuteration, this band shows a lower frequency shift of about

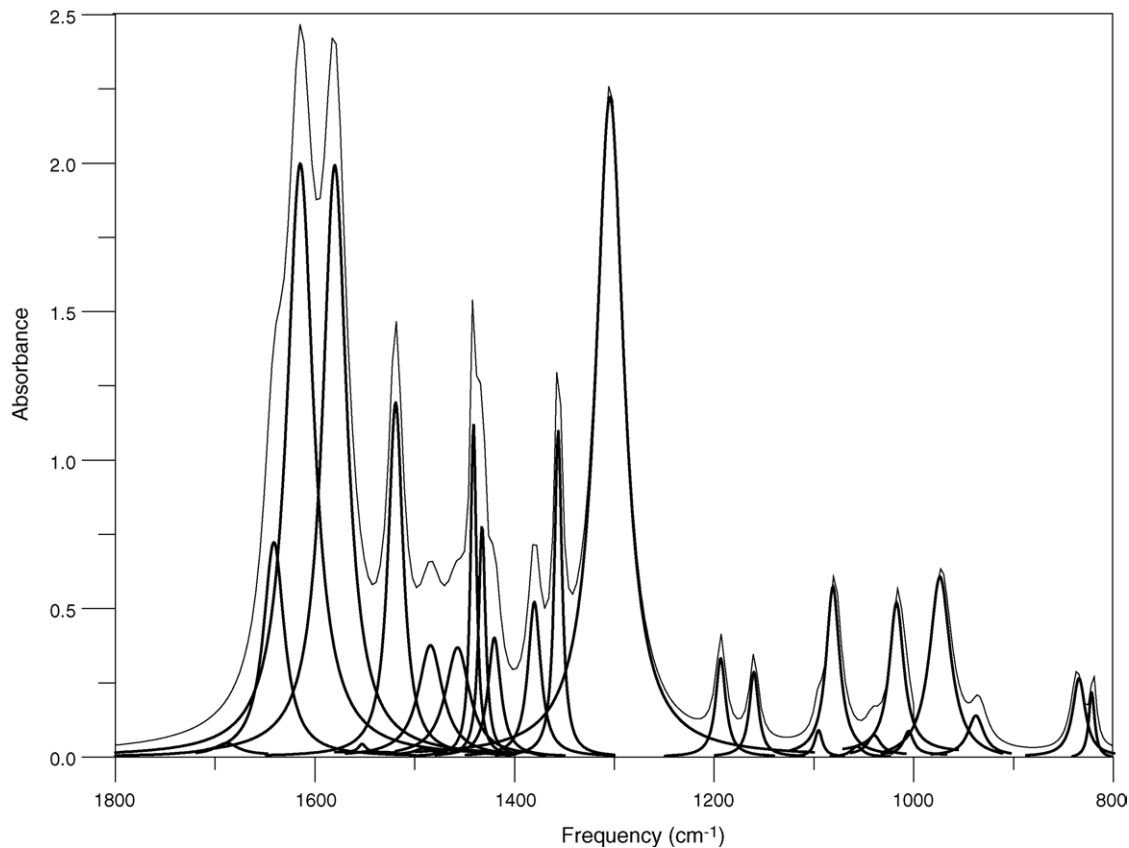


Fig. 5. Deconvoluted infrared spectrum of MeAPO in CCl_4 in 1800–800 cm^{-1} region, the experimental spectra (top) and the results of fitting (bottom).

Table 4
Fundamental band assignment of MeAPO^a

	Theoretical ^b			Infrared		Raman	Assignment
	Frequencies	IR, <i>I</i>	R, <i>I</i>	Solid	CCl ₄	Solid	
1	3321	36	24	3167(m)	3171(6)	3165(6)	νNM
2	3219	2	33	3067(w)	3077(11)	3079(11)	νCH _α
3	3159	3	25	3012(vw)	3014(5)	3013(10)	ν ₃ CH ₃
4	3147	5	36	2997(w)	3000(11)	2999(3)	ν ₄ CH ₃
5	3140	6	33	2997(w)	3000(11)	2999(3)	ν ₄ CH ₃
6	3120	4	54	2984(w)	2986(3)	2987(6)	ν ₄ CH ₃
7	3097	4	43	2967(w)	2969(3)	2965(sh)	ν ₄ CH ₃
8	3072	10	46	2934(w)	2935(19)	2937(3)	ν ₄ CH ₃
9	3056	3	100	2917(vw)	2920(3)	2915(58)	ν ₅ CH ₃
10	3049	6	91	2917(vw)	2920(3)	2915(58)	ν ₅ CH ₃
11	3027	20	94	2889(w)	2894(9)	2885(sh)	ν ₅ CH ₃
12	1687	100	33	1635(sh)	1641(32)	1633(7)	ν ₂ C=C—C=O + δNH
13	1662	92	12	1615(s)	1615(90)	1617(22)	ν ₃ C=C—C=O + δNH
14	1567	26	19	1565(s)	1580(90)	1560(12)	ν ₂ C=C—C—N + δCH
15	1537	3	9	1521(m)	1519(54)	1520(65)	δ _a CH ₃
16	1526	4	7	1489(w)	1484(17)	1488(5)	δ _a CH ₃
17	1513	11	1	1461(m)	1457(17)	1463(21)	δ _a CH ₃ + δNH
18	1510	5	12	1461(m)	1457(17)	1464(21)	δ _a CH ₃
19	1507	10	17	1453(sh)	1441(50)	1450(5)	δ _a CH ₃
20	1505	1	6	1453(sh)	1441(50)	1450(5)	δ _a CH ₃
21	1493	5	21	1434(ms)	1432(35)	1438(10)	δ _s CH ₃
22	1441	3	8	1423(m)	1420(18)	1425(5)	δ _s CH ₃
23	1417	6	12	1380(ms)	1380(23)	1380(17)	δ _s CH ₃
24	1384	55	9	1349(s)	1356(49)	1341(16)	ν ₂ C=C—C + δNH
25	1327	38	12	1291(s)	1304(100)	1293(32)	ν ₃ C=C—C + δCH _α
26	1233	7	3	1195(mw)	1193(15)	1200(30)	δCH _α
27	1200	2	1	1152(w)	1160(13)	1156(19)	νN—CH ₃ + ρCH ₃
28	1157	0.1	1.5	1106(sh)	1095(4)	1105(6)	πCH ₃
29	1119	6	1	1069(s)	1079(26)	1074(10)	δNH + ρCH ₃
30	1075	0.1	0.3	1039(w)	1041(3)	1038(5)	πCH ₃
31	1055	4	0.5	1015(ms)	1016(23)	1014(15)	πCH ₃
32	1045	2	2	1005(sh)	1007(4)	1004(sh)	ρCH ₃
33	1009	6	3	968(ms)	972(28)	970(8)	ρCH ₃
34	947	1	1	930(m)	934(6)	936(18)	ν ₂ C—CH ₃ + δC—C=O + δCH
35	857	0.1	3	859 (sh)	836(12)	852(sh)	νC—CH ₃ + δC=C—N + δCH
36	814	13	1	827(s)	820(10)	831(39)	(γNH + γCH) out of phase
37	745	12	1	730(s)	*	726(19)	(γNH + γCH) in phase
38	655	3	4	650(m)	650(14)	655(100)	Δ + δC—CH ₃
39	647	—	0.1	635(vw)	628(6)	637(10)	Γ
40	551	0.3	1	555(mw)	543(3)	558(26)	Γ
41	536	1	3	535(m)	531(9)	534(53)	Δ + δC—CH ₃
42	398	2	2	415(m)	420(3)	412(11)	ν _{as} N···O + δC—CH ₃
43	372	1	2	n.m.	n.m.	389(72)	Δ + δC—CH ₃
44	291	0.3	0.3	n.m.	n.m.	309(18)	Δ + δC—CH ₃
45	211	0.3	1	n.m.	n.m.	234(34)	Γ + γC—CH ₃
46	195	0.1	1	n.m.	n.m.	221(16)	Δ + δC—CH ₃
47	193	1	0.3	n.m.	n.m.	201(sh)	Δ + δC—CH ₃
48	147	—	—	n.m.	n.m.	179(75)	Γ + γC—CH ₃
49	113	1	0.1	n.m.	n.m.	n.m.	τCH ₃
50	68	1	0.05	n.m.	n.m.	n.m.	τCH ₃
51	29	0.5	0.1	n.m.	n.m.	n.m.	τCH ₃

Frequencies are in cm⁻¹ and intensities are relative.

^a IR, infrared; R, Raman; *I*, calculated relative intensity; ν, stretching; δ, in plane bending; γ, out of plane bending; ρ, rocking in plane; π, rocking out of plane Δ, in plane ring deformation; Γ, out of plane ring deformation; v, very; s, strong; m, medium; w, weak; sh, shoulder; τ, torsion; n.m., not measured; *, solvent overlapped, relative intensities are given in parentheses.

^b Unscaled frequencies, calculated at B3LYP/6-31G** level.

Table 5
Fundamental band assignment of DMeAPO^a

	Theoretical ^b			Infrared		Raman	Assignment
	Frequencies	IR, <i>I</i>	R, <i>I</i>	Solid	CCl ₄	Solid	
1	3219	2	33	3066(w)	3076(8)	3078(20)	νCH_α
2	3159	2	25	3013(vw)	3015(5)	3014(43)	$\nu_a\text{CH}_3$
3	3148	4	37	2997(w)	2999(10)	3000(50)	$\nu_a\text{CH}_3$
4	3139	5	32	2997(w)	2999(10)	3000(50)	$\nu_a\text{CH}_3$
5	3120	3	54	2983(w)	2986(3)	2986(sh)	$\nu_a\text{CH}_3$
6	3099	3	44	2966(w)	2968(3)	2963(92)	$\nu_a\text{CH}_3$
7	3072	8	46	2935(w)	2936(18)	2938(42)	$\nu_a\text{CH}_3$
8	3056	2	100	2917(w)	2919(32)	2917(75)	$\nu_s\text{CH}_3$
9	3049	4	91	2917(w)	2919(32)	2917(15)	$\nu_s\text{CH}_3$
10	3028	15	91	2888(w)	2893(32)	2887(3)	$\nu_s\text{CH}_3$
11	2442	20	11	2275(mw)	2286(6)	2278(14)	νND
12	1684	52	6	1631(s)	1635(100)	1630(22)	$\nu_a\text{C}=\text{C}-\text{C}=\text{O}$
13	1585	100	15	1575(m)	1571(37)	1568(8)	$\nu_s\text{C}=\text{C}-\text{C}=\text{O} + \delta\text{ND}$
14	1564	23	20	1556(m)	1563(6)	1554(3)	$\nu_a\text{C}-\text{C}=\text{C}-\text{N} + \delta\text{CH}$
15	1537	2	10	1518(w)	1520(93)	1522(5)	$\delta_a\text{CH}_3$
16	1526	2	7	1486(w)	1457(8)	1484(90)	$\delta_a\text{CH}_3$
17	1511	11	11	1462(m)	1457(8)	1462(25)	$\delta_a\text{CH}_3$
18	1507	0.4	17	1462(m)	1457(8)	1462(25)	$\delta_a\text{CH}_3$
19	1505	1	6	1451(mw)	1442(10)	1451(sh)	$\delta_a\text{CH}_3$
20	1502	14	5	1451(mw)	1441(10)	1451(sh)	$\delta_a\text{CH}_3$
21	1484	23	14	1436(ms)	1419(45)	1434(20)	$\delta_s\text{CH}_3$
22	1440	0.2	10	1423(m)	1419(45)	1423(12)	$\delta_s\text{CH}_3$
23	1417	4	12	1384(s)	1379(11)	1380(30)	$\delta_s\text{CH}_3$
24	1326	37	11	1310(w)	1314(15)	1311(10)	$\nu_a\text{C}\cdots\text{C}\cdots\text{C} + \delta\text{CH}_\alpha$
25	1272	5	2	1231(s)	1247(55)	1239(3)	$\nu_s\text{C}\cdots\text{C}\cdots\text{C} + \delta\text{CH} + \delta\text{ND}$
26	1207	6	2	1153(ms)	1194(56)	1170(15)	$\delta\text{CH}_\alpha + \delta\text{ND}$
27	1185	0.1	1	1135(vw)	1138(7)	1134(2)	$\nu\text{N}-\text{CH}_3 + \rho\text{CH}_3$
28	1153	–	1	1069(ms)	1095(7)	1099(2)	πCH_3
29	1075	0.2	0.2	1038(vw)	1041(6)	1040(70)	πCH_3
30	1055	3	0.5	1016(m)	1015(10)	1015(3)	πCH_3
31	1049	2	2.5	1004(w)	1005(5)	1007(2)	ρCH_3
32	1011	2	3	1000(vw)	975(6)	977(4)	ρCH_3
33	961	3	1	960(w)	950(10)	955(2)	$\delta\text{ND} + \nu\text{N}-\text{CH}_3$
34	946	0.3	1	940(m)	942(15)	940(27)	$\nu_a\text{C}-\text{CH}_3 + \delta\text{C}=\text{C}-\text{O} + \delta\text{CH}$
35	850	0.2	3	842(mw)	830(8)	845(41)	$\nu\text{C}-\text{CH}_3 + \delta\text{C}=\text{C}-\text{N} + \delta\text{CH}$
36	756	1.5	1	734(mw)	*	735(4)	γCH_α
37	677	6	0.1	–	660(15)	675(4)	γND
38	652	2	5	651(m)	648(10)	652(100)	$\Delta + \delta\text{C}-\text{CH}_3$
39	580	3	1	672(mw)	560(4)	575(27)	Γ
40	533	1	3	571(w)	530(5)	532(65)	$\Delta + \delta\text{C}-\text{CH}_3$
41	529	2	1	533(w)	505(14)	515(5)	Γ
42	397	1.5	2	412(m)	431(1)	408(sh)	$\nu_a\text{NDO} + \delta\text{C}-\text{CH}_3$
43	370	1	1.5	n.m.	n.m.	386(75)	$\Delta + \delta\text{C}-\text{CH}_3$
44	291	0.2	0.2	n.m.	n.m.	309(3)	$\Delta + \delta\text{C}-\text{CH}_3$
45	211	0.2	1	n.m.	n.m.	231(24)	$\Delta + \delta\text{C}-\text{CH}_3$
46	194	0.2	0.7	n.m.	n.m.	221(sh)	$\Delta + \delta\text{C}-\text{CH}_3$
47	191	1	0.3	n.m.	n.m.	199(5)	$\Delta + \delta\text{C}-\text{CH}_3$
48	146	–	–	n.m.	n.m.	180(63)	$\Gamma + \gamma\text{C}-\text{CH}_3$
49	113	0.5	0.1	n.m.	n.m.	n.m.	τCH_3
50	67	0.7	0.1	n.m.	n.m.	n.m.	τCH_3
51	29	0.4	0.1	n.m.	n.m.	n.m.	τCH_3

Frequencies are in cm^{-1} and intensities are relative.

^a IR, infrared; R, Raman; *I*, calculated relative intensity; ν , stretching; δ , in plane bending; γ , out of plane bending; ρ , rocking in plane; π , rocking out of plane Δ , in plane ring deformation; Γ , out of plane ring deformation; ν , very; *s*, strong; *m*, medium; *w*, weak; *sh*, shoulder; π , torsion; *n.m.*, not measured; *, solvent overlapped, relative intensities are given in parentheses.

^b Unscaled Frequencies, calculated at B3LYP/6-31G** level.

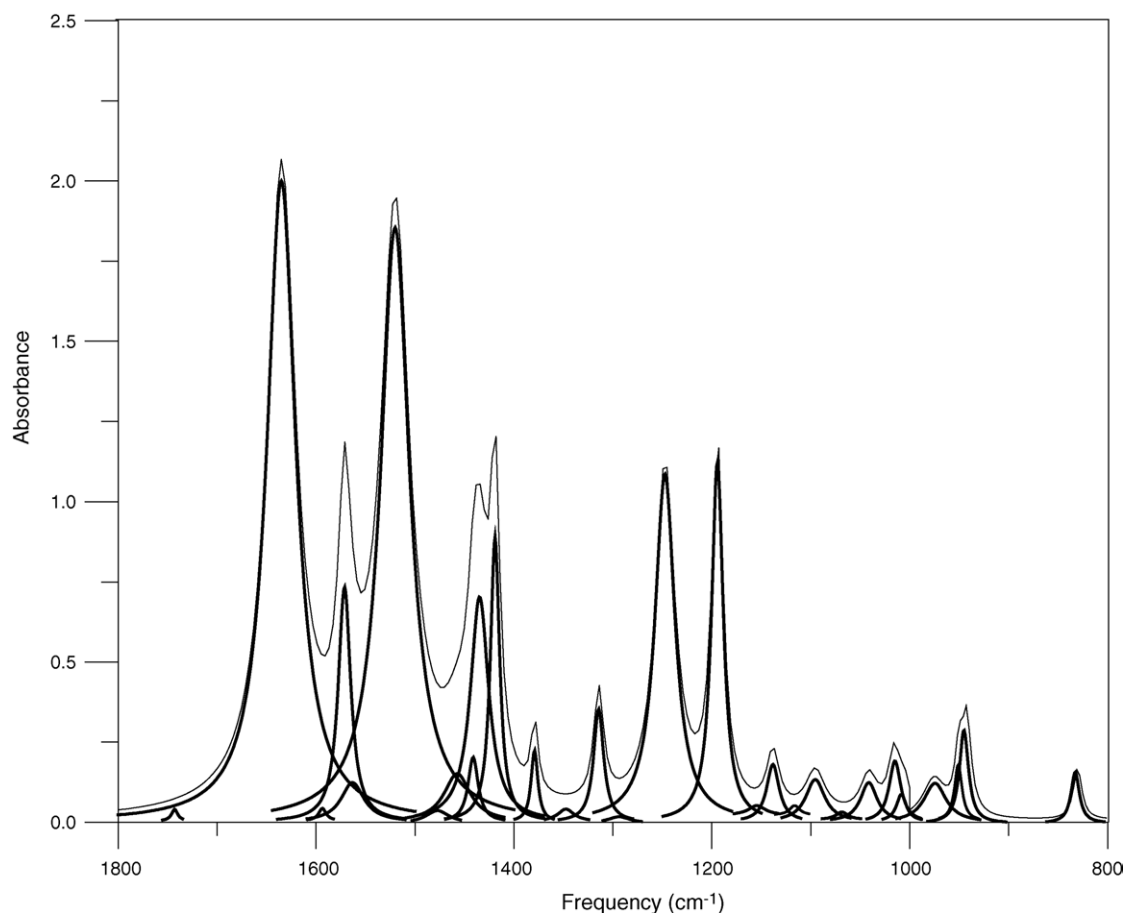


Fig. 6. Deconvoluted infrared spectrum of DMeAPO in CCl_4 in $1800\text{--}800\text{ cm}^{-1}$ region, the experimental spectra (top) and the results of fitting (bottom).

4 cm^{-1} , which is in close agreement with the theoretically calculated, 3 cm^{-1} frequency shift (calculated at B3LYP/6-31G**). Therefore, we assign the band at about 1630 cm^{-1} in DMeAPO to $\nu_a\text{C}=\text{C}=\text{C}=\text{O}$. The infrared spectrum of MeAPO shows a strong band at about 1615 cm^{-1} . The corresponding Raman band appears as a medium band at 1617 cm^{-1} . In DMeAPO, this band shifts toward lower frequencies and appears at about 1570 cm^{-1} . The corresponding band in APO, which occurs at 1605 cm^{-1} , upon deuteration shifts downward about 50 cm^{-1} [2]. Theoretical calculations suggest that this band is due to the symmetric $\text{C}=\text{C}=\text{C}=\text{O}$ stretching which is strongly coupled to δNH .

The strong infrared band at 1565 cm^{-1} in the solid phase moves to 1580 cm^{-1} in solution. The upper frequency shift of this band in solution (15 cm^{-1}) suggests more stretching character for this band. According to the DFT calculations, this band is mainly due to the asymmetric $\text{C}=\text{C}=\text{C}=\text{N}$ stretching which is coupled to CH_α in plane bending mode. Another strong IR band in this region is a band at about 1350 cm^{-1} . The corresponding Raman band appears as a medium band at 1341 cm^{-1} . By the help of the theoretical calculations and intensity considering we assign this band to asymmetric $\text{C}=\text{C}=\text{C}$ stretching mode coupled to $\text{N}=\text{H}$ in plane bending mode. Upon deuteration, this band shifts to 1310 cm^{-1} and,

according to the calculations, its coupling to δND is completely removed. In the case of DMeAPO, this band is coupled mainly to the δCH_α . The strong infrared and Raman band at about 1290 cm^{-1} assigned to symmetric $\text{C}=\text{C}=\text{C}$ stretching mode which is coupled to δCH_α . An increase in the frequency of this band by going from solid to CCl_4 solution also suggests that this band has mainly a stretching character. In DMeAPO, this band considerably shifts to lower frequencies and appears at about 1240 cm^{-1} with a decrease in its Raman intensity. According to the theoretical calculations, this band is due to the symmetric $\text{C}=\text{C}=\text{C}$ stretching + δCH_α which is strongly coupled to δND . The decrease in the Raman intensity of this band upon deuteration is due to decreased $\nu_s\text{C}=\text{C}=\text{C}$ character of the vibration and strongly coupled the calculated results. The corresponding band in APO also shows a down shift of about 20 cm^{-1} upon deuteration. It should be mentioned that this band in APO and its deuterated analogous is assigned mainly to $\nu_s\text{C}=\text{C}=\text{C}=\text{N}$ [2]. The change in the vibrational mode of this band could be attributed to the more band equalization in the chelated ring due to the stronger H bond in MeAPO than that APO. According to the ab initio calculations (at B3LYP/6-311++G** level), the $\text{C}_2\text{--C}_3$ and $\text{N}_7\text{--C}_4$ distances in MeAPO are shorter than those in APO (0.006 , 0.001 \AA , respectively) but the $\text{C}_3=\text{C}_4$ and $\text{C}_2=\text{O}_6$ distances

Table 6

All calculated frequencies at different levels and basis sets

	B3LYP/6- 31G**	B3LYP/6- 31G*	B3LYP/6- 311++G**	B1LYP/6- 311++G**	G96LYP/6- 311++G**	B1LYP/6- 31G**	B1LYP/6- 31G*	B3PW91/6- 31G**	G96LYP/6- 31G**	G96LYP/6- 31G*	MP2/6- 31G*
1	3319	3347	3347	3392	3168	3371	3420	3295	3137	3146	3447
2	3217	3218	3198	3212	3123	3230	3222	3228	3102	3134	3256
3	3158	3159	3136	3145	3062	3170	3172	3174	3080	3078	3227
4	3142	3149	3124	3134	3050	3154	3170	3166	3065	3066	3221
5	3141	3140	3116	3126	3045	3154	3159	3158	3061	3057	3217
6	3119	3120	3096	3105	3021	3130	3116	3135	3040	3036	3186
7	3099	3099	3077	3088	2999	3110	3111	3118	3020	3016	3179
8	3068	3073	3053	3064	2980	3081	3085	3083	2987	2987	3161
9	3051	3055	3035	3044	2964	3062	3062	3057	2976	2977	3104
10	3045	3049	3030	3041	2956	3057	3060	3055	2971	2971	3104
11	3020	3028	3009	3021	2939	3033	3040	3027	2943	2947	3091
12	1686	1691	1660	1671	1599	1699	1712	1700	1622	1631	1731
13	1662	1669	1626	1637	1558	1672	1683	1674	1590	1596	1695
14	1562	1567	1547	1554	1496	1570	1572	1573	1510	1516	1598
15	1521	1536	1508	1517	1469	1531	1546	1515	1482	1496	1571
16	1510	1526	1499	1506	1462	1520	1534	1504	1474	1490	1557
17	1499	1516	1487	1496	1451	1509	1525	1491	1464	1481	1549
18	1495	1511	1481	1490	1446	1504	1517	1489	1459	1474	1538
19	1490	1506	1479	1488	1445	1499	1515	1482	1455	1471	1535
20	1488	1505	1474	1483	1440	1497	1509	1479	1453	1470	1534
21	1479	1492	1466	1475	1425	1488	1502	1471	1437	1450	1521
22	1426	1442	1415	1424	1377	1436	1452	1420	1388	1404	1468
23	1402	1418	1389	1398	1349	1411	1418	1392	1363	1379	1437
24	1380	1396	1367	1374	1325	1389	1408	1379	1337	1353	1424
25	1321	1326	1309	1315	1268	1327	1329	1326	1279	1284	1351
26	1227	1235	1219	1226	1178	1235	1241	1227	1186	1194	1258
27	1193	1201	1184	1191	1142	1201	1209	1196	1151	1159	1226
28	1148	1156	1139	1146	1104	1156	1164	1144	1114	1122	1178
29	1115	1122	1106	1111	1070	1120	1127	1119	1080	1088	1139
30	1064	1075	1058	1065	1028	1071	1081	1057	1034	1045	1086
31	1044	1055	1039	1047	1007	1051	1056	1038	1011	1023	1065
32	1038	1047	1034	1039	1004	1045	1053	1032	1009	1018	1062
33	1002	1009	997	1002	962	1007	994	996	969	976	1010
34	946	947	940	944	909	950	951	952	914	915	963
35	856	857	848	852	817	859	853	863	825	825	867
36	816	803	809	800	810	808	786	835	824	805	748
37	751	748	756	755	730	753	744	750	731	730	686
38	655	657	653	656	636	660	664	663	632	635	671
39	645	646	647	649	628	646	635	640	626	627	606
40	551	551	554	557	534	554	551	549	532	532	546
41	536	537	537	539	519	539	544	537	519	520	530
42	400	400	396	396	386	401	399	400	390	391	399
43	373	374	372	372	359	374	366	370	361	363	370
44	292	292	292	292	276	294	289	289	279	279	296
45	212	212	211	208	204	212	204	209	208	207	209
46	198	200	197	190	183	197	195	197	188	196	199
47	195	197	192	187	171	195	186	193	186	186	185
48	150	149	148	145	146	150	149	150	147	146	147
49	104	103	104	99	94	103	100	98	101	101	93
50	61	56	58	50	35	58	39	55	56	51	8
51	36	34	23	38	31	22	18	35	27	24	5

are longer in MeAPO, than the corresponding bond length in APO (0.001, 0.005 Å, respectively). The corresponding band in the deuterated analogue is coupled to the ND in plane bending mode, which explains the frequency shift upon deuteration.

The Raman spectrum of MeAPO shows a medium band at 1074 cm⁻¹. The corresponding IR band appears as a strong band and upon deuteration disappears. According to the the-

oretical calculations this band is mainly due to the NH in plane bending mode, which is coupled to ρ CH₃. In the case of DMeAPO, this mode is coupled mainly to the ν C-CH₃ and appears, as it is predicted by calculations, at around 960 cm⁻¹.

By considering the theoretical calculations and comparing with the spectra of APO [2], the bands at about 1520, 1490, 1461, 1450, 1435, 1420 and 1380 cm⁻¹ were assigned

to the CH₃ deformation modes and the band at about 1195 was assigned to the olefinic CH in plane bending mode. The bands at about 1105, 1040, 1015 and 1005 cm⁻¹ are assigned mainly to the CH₃ rocking modes.

4.3.3. Below 1000 cm⁻¹

In this region, we expect to observe C–CH₃ stretching, C₃C₂O₆ and C₃C₄N₇ deformations, N–H and C–H_α out of plane bending modes and in plane and out of plane ring deformation modes.

Theoretical calculations suggest that the band at about 930 cm⁻¹ is due to asymmetric C–CH₃ stretching mode, which is somewhat, coupled to the in plane C₃–C₂=O₆ and CH_α bending modes. Upon deuteration this band shows an upward frequency shift of about 10 cm⁻¹. The corresponding band in APO (980 cm⁻¹) [2] shows also an upward frequency shift upon deuteration. The infrared band at 859 cm⁻¹ shows a downward frequency shift upon deuteration, which is in agreement with our theoretical calculations, we assign this band to the C–CH₃ stretching mode coupled to the in plane C₃–C₄–N₇ and CH_α bending modes.

The vibrational spectra of MeAPO indicate two bands at about 830 and 730 cm⁻¹, which the former completely disappear in DMeAPO. According to our calculations, these two bands are caused by (γNH₁₀ + γCH_α) out of phase, and in phase, respectively. In DMeAPO, decoupling of γCH_α and γND₁₀ causes that these two bands to be observed at 675 and 735 cm⁻¹, respectively, which is in agreement with the calculated results. In the case of APO, the out of plane NH₁₀ bending mode appears at lower frequencies (755 cm⁻¹) than that for MeAPO (830 cm⁻¹). This frequency shift also supports the presence of stronger hydrogen bond in MeAPO compared to that in APO and very well agrees with the NMR proton chemical shift.

It is noteworthy that the frequencies of the in plane ring deformation modes in MeAPO are considerably higher than the corresponding modes in APO. This could be attributed to the stronger ring in MeAPO in comparison with APO, which is caused by stronger hydrogen bond and more π-electron delocalization in the former. The 620 cm⁻¹ band in APO appear at 650 cm⁻¹ in MeAPO and the 462 cm⁻¹ band in the former appear at 535 cm⁻¹ in the latter.

It is interesting to consider the frequency shift of out of plane ring deformation mode at 635 cm⁻¹ upon deuteration. This frequency shift is caused by coupling of this mode with γNH/γND and is predicted correctly by the theoretical calculations. The medium to strong Raman band at 558 cm⁻¹ corresponds to another out of plane ring deformation mode. The theoretical calculation predicts that this band shifts toward lower frequencies in DMeAPO, which is in agreement with the experimental observations. The Raman bands at about 390 and 310 cm⁻¹ are also assigned to the in plane ring deformation modes, which are coupled to δC–CH₃. According to our calculations, the bands at 234 and 179 cm⁻¹ are assigned to out of plane ring deformation modes coupled to γC–CH₃.

The N···O stretching mode in the APO spectrum at 360 cm⁻¹ also shows considerable upward frequency shift (412 cm⁻¹) by CH₃ substitution on the Nitrogen atom. This frequency shift also supports the presence of stronger hydrogen bond in MeAPO compared to that in APO.

5. Conclusion

The structure, intramolecular hydrogen and vibrational spectra of MeAPO have been measured and analyzed by the aid of calculations at the density functional theory (DFT) levels and post-Hartree–Fock (MP2) level and considering its spectral behaviors upon deuteration. Superior results were obtained with B3LYP/6-31G**. All theoretical calculations and experimental results reveal that the intramolecular H-bond by methyl substitution on the Nitrogen atom of APO become stronger than that APO.

Theoretical calculations show that the hydrogen of NHCH₃ group is in the plane of the chelated ring. Analysis of the vibrational spectra indicates strong coupling between the chelated ring modes.

References

- [1] S.F. Tayyari, H. Raissi, F. Tayyari, Spectrosc. Chim. Acta Part A 58 (2002) 1681.
- [2] H. Raissi, S.F. Tayyari, F. Tayyari, J. Mol. Struct. 613 (2002) 195.
- [3] S.F. Tayyari, H. Raissi, F. Milani-Nejad, I.S. Butler, Vib. Spectrosc. 26 (2001) 187.
- [4] V. Barone, P. Palma, N. Sanna, Phys. Lett. 381 (2003) 451.
- [5] S.L. Quan, W. Fang, Phys. Lett. 367 (2003) 637.
- [6] A. Masad, D. Huppert, Chem. Phys. Lett. 180 (1991) 409.
- [7] J.C. Jiang, M.H. Tsai, J. Phys. Chem. A 101 (1997) 1982.
- [8] S.D. Choudhurg, S. Basu, Chem. Phys. Lett. 371 (2003) 136.
- [9] P. Kakkar, V. Katoch, J. Mol. Struct. (Theochem.) 578 (2002) 169.
- [10] A. Grofsik, M. Kubinyi, A. Ruzsinszky, T. Veszpremi, W.J. Jones, J. Mol. Struct. 555 (2000) 15.
- [11] G.A. Jeffery, W. Sanger, Hydrogen Bonding in Biological Structure, Springer, Berlin, 1991.
- [12] K. Rutkowski, A. Koll, J. Mol. Struct. 322 (1994) 195.
- [13] H. Lampert, M. Mikenda, A. Karpfen, J. Phys. Chem. 100 (1996) 7418.
- [14] A. Simperler, W. Mikenda, Monatsh. Chem. 128 (1997) 969.
- [15] K.B. Borisenko, C.W. Bock, I. Hargittai, J. Phys. Chem. 100 (1996) 7426.
- [16] A. Kovacs, I. Mascari, I. Hargittai, J. Phys. Chem. A 103 (1999) 3110.
- [17] A. Kovacs, I. Hargittai, Struct. Chem. 11 (2000) 193.
- [18] M. Cuma, S. Scheiner, T. Kar, J. Am. Chem. Soc. 120 (1998) 10499.
- [19] M. Cuma, S. Scheiner, T. Kar, J. Mol. Struct. (Theochem.) 467 (1999) 37.
- [20] G. Chung, O. Kwon, Y. Kwon, J. Phys. Chem. A 102 (1998) 2381.
- [21] A. Koll, Bull. Soc. Chim. Belg. 92 (1983) 313.
- [22] A. Koll, P. Wolschann, Monatsh. Chem. 127 (1996) 475.
- [23] A. Koll, P. Wolschann, Monatsh. Chem. 130 (1999) 983.
- [24] S.F. Tayyari, F. Milani-Nejad, M. Fazli, J. Mol. Struct. (Theochem.) 541 (2001) 11.
- [25] D. Smith, P.J. Taylor, Spectrochim. Acta 32A (1976) 1477.
- [26] M.C. Ether, J. Phys. Chem. 95 (1991) 4601.
- [27] G.R. Desiraju, Angew. Chem., Int. Ed. Engl. 34 (1995) 2311.

- [28] J. Bernstein, R.E. Davis, L. Shimoni, N.L. Chang, *Angew. Chem., Int. Ed. Engl.* 34 (1995) 1555.
- [29] Z. Yoshida, H. Ogoshi, T. Tokomitsu, *Tetrahedron* 26 (1970) 5691.
- [30] J. Emsley, L.Y.Y. Ma, S.C. Nyburg, A.W. Parkins, *J. Mol. Struct.* 240 (1990) 59.
- [31] B. Schiøtt, B.B. Iversen, G.K.H. Madsen, T. Bruice, *J. Am. Chem. Soc.* 120 (1998) 12117.
- [32] J. Weinstein, G.M. Wyman, *J. Org. Chem.* 23 (1958) 1618.
- [33] M.J. Frisch, A.C. Scheiner, H.F. Schaefer, J.S. Binkly, *J. Chem. Phys.* 82 (1985) 4194.
- [34] M.J. Frisch, G.W. Trucks, H.B. Schlegel, G.E. Scuseria, M.A. Robb, J.R. Cheeseman, V.G. Zakrzewski, J.A. Montgomery Jr., R.E. Stratmann, J.C. Burant, S. Dapprich, J.M. Millam, A.D. Daniels, K.N. Kudin, M.C. Strain, O. Farkas, J. Tomasi, V. Barone, M. Cossi, R. Cammi, B. Mennucci, C. Pomelli, C. Adamo, S. Clifford, J. Ochterski, G.A. Petersson, P.Y. Ayala, Q. Cui, K. Morokuma, D.K. Malick, A.D. Rabuck, K. Raghavachari, J.B. Foresman, J. Cioslowski, J.V. Ortiz, B.B. Stefanov, G. Liu, A. Liashenko, P. Piskorz, I. Komaromi, R. Gomperts, R.L. Martin, D.J. Fox, T. Keith, M.A. Al-Laham, C.Y. Peng, A. Nanayakkara, C. Gonzalez, M. Challacombe, P.M.W. Gill, B. Johnson, W. Chen, M.W. Wong, J.L. Andres, C. Gonzalez, M. Head-Gordon, E.S. Replogle, J.A. Pople, Gaussian 98, Revision A.6, Gaussian, Inc., Pittsburgh, PA, 1998.
- [35] A.D. Becke, *Phys. Rev. B* 38 (1988) 3098.
- [36] A.D. Becke, *J. Chem. Phys.* 98 (1993) 5648.
- [37] J.P. Perdew, Y. Wang, *Phys. Rev. B* 45 (1992) 13244.
- [38] C. Lee, W. Yang, R.G. Parr, *Phys. Rev. B* 37 (1988) 875.
- [39] V. Bertolasi, P. Gilli, V. Forreti, C. Gilli, *J. Am. Chem. Soc.* 113 (1991) 4917.
- [40] J.T. Pelton, L.R. McLean, *Anal. Biochem.* 277 (2000) 167.
- [41] T.K. Nadler, S.T. McDaniel, M.O. Westerhaus, J.S. Shenk, *Appl. Spectrosc.* 43 (1989) 1354.